B978-0-08-100355-8.00007-2, 00007

AUTHOR QUERY FORM

ELSEVIER	**Book: Developments in Clay Science** **Article Number: 7**	**Please e-mail your responses and any corrections to:** **E-mail: M.Bernard@elsevier.com**

Dear Author,

Please check your proof carefully and mark all corrections at the appropriate place in the proof (e.g., by using on-screen annotation in the PDF file) or compile them in a separate list. Note: if you opt to annotate the file with software other than Adobe Reader then please also highlight the appropriate place in the PDF file. To ensure fast publication of your paper please return your corrections within 48 hours.

For correction or revision of any artwork, please consult http://www.elsevier.com/artworkinstructions.

We were unable to process your file(s) fully electronically and have proceeded by

☐ Scanning (parts of) your article ☐ Rekeying (parts of) your article ☐ Scanning the artwork

Any queries or remarks that have arisen during the processing of your manuscript are listed below and highlighted by flags in the proof. Click on the '**Q**' link to go to the location in the proof.

Location in Chapter	**Query / Remark: click on the Q link to go** **Please insert your reply or correction at the corresponding line in the proof**
Q1	As per the specifications, a credit line is always preceded by anyone of the following terms: "Reproduced with permission from", "From", "Modified from", "Data from", "Based on" or "Courtesy" instead of the term "Redrawn from" in the figure captions.
Q2	Please check whether the suggested running head "Applications of NIR/MIR to Determine Site Occupancy" is appropriate for this chapter.
Q3	Please check the author affiliations, and correct if necessary.

B978-0-08-100355-8.00007-2, 00007

Q4	Please check the keywords that the copyeditor has assigned, and correct if necessary.
Q5	Please check the symbol "□", and correct if necessary.
Q6	The citation "Serna et al. 1977" has been changed to match the author name/date in the reference list. Please check here and in subsequent occurrences, and correct if necessary.
Q7	The citation "Brigatti et al. 2013" has been changed to match the author name/date in the reference list. Please check here and in subsequent occurrences, and correct if necessary.
Q8	The citation "Stathopoulou et al., 2001" has been changed to match the author name/date in the reference list. Please check here and in subsequent occurrences, and correct if necessary.
Q9	The citation "Petit et al., 1999" has been changed to match the author name/date in the reference list. Please check here and in subsequent occurrences, and correct if necessary.
Q10	The citation "Muller (1991)" has been changed to match the author name/date in the reference list. Please check here and in subsequent occurrences, and correct if necessary.
Q11	The citation "Zviagina (2004)" has been changed to match the author name/date in the reference list. Please check here and in subsequent occurrences, and correct if necessary.
Q12	The citation "Petit et al., (2004)" has been changed to match the author name/date in the reference list. Please check here and in subsequent occurrences, and correct if necessary.
Q13	The citation "Baron et al., 2016" has been changed to match the author name/date in the reference list. Please check here and in subsequent occurrences, and correct if necessary.
Q14	Citation "Petit et al., 1997" has not been found in the reference list. Please supply full details for this reference.
Q15	The citation "Decarreau et al. 1987" has been changed to match the author name/date in the reference list. Please check here and in subsequent occurrences, and correct if necessary.

B978-0-08-100355-8.00007-2, 00007

Q16	The citation "Kloprogge et al., 1990" has been changed to match the author name/date in the reference list. Please check here and in subsequent occurrences, and correct if necessary.
Q17	The citation "2006" has been changed to match the author name/date in the reference list. Please check here and in subsequent occurrences, and correct if necessary.
Q18	The citation "Baron et al. 2016" has been changed to match the author name/date in the reference list. Please check here and in subsequent occurrences, and correct if necessary.
Q19	The citation "Frost et al., 2001" has been changed to match the author name/date in the reference list. Please check here and in subsequent occurrences, and correct if necessary.
Q20	The citation "Yan et al., 1996" has been changed to match the author name/date in the reference list. Please check here and in subsequent occurrences, and correct if necessary.
Q21	The citation "Chryssikos et al. 2007" has been changed to match the author name/date in the reference list. Please check here and in subsequent occurrences, and correct if necessary.
Q22	The citation "Farmer (1974)" has been changed to match the author name/date in the reference list. Please check here and in subsequent occurrences, and correct if necessary.
Q23	The citation "Ferranti et al., 2015" has been changed to match the author name/date in the reference list. Please check here and in subsequent occurrences, and correct if necessary.
	Please check this box or indicate your approval if you have no corrections to make to the PDF file ☐

Thank you for your assistance.

B978-0-08-100355-8.00007-2, 00007

Chapter 7

C0035 # Applications of NIR/MIR to Determine Site Occupancy in Smectites

Will P. Gates*,[1], Sabine Petit[†] and Jana Madejová[‡]

*Deakin University, Melbourne, VIC, Australia

†Institut de Chimie des Milieux et Matériaux de Poitiers, Poitiers, France

‡Institute of Inorganic Chemistry, Bratislava, Slovakia

[1]Corresponding author: e-mail: gateswp@smectech.com.au

Q3

s0005 7.1 INTRODUCTION

p0005 This chapter will show how vibrational spectroscopy, in particular, near infrared (NIR) and mid infrared (MIR) spectra, in combination with chemical and other physical data can successfully be used to assist in the determination of site occupancies by different ions in clay minerals. Traditional approaches for determining structural chemistry of clay minerals, as emphasised herein, are still the norm. However, there is no real impediment to the implementation of multivariate and chemometric methods of analysis other than the issue of sample size.

p0010 The accurate and precise assignment of ions (cations and anions) within distinct octahedral and tetrahedral sites of the smectite structure continues to remain an important focus for some researchers where IR and Raman spectroscopies play a key role. In natural smectites, Si, often Al and sometimes Fe^{3+}, occupy tetrahedral sites and Al, Mg, Fe^{3+}, as well as Fe^{2+}, Ni^{2+}, Zn^{2+} and Li^{+} occupy octahedral sites within the structure. Chemical analyses, in combination with X-ray powder diffraction and other methods, has enabled smectites to be differentiated based on the occupancies of the tetrahedral and octahedral sites, but because of the small particle size and the poorly crystalline nature of smectites, only average, bulk information is available. The use of alternative techniques, including IR and Raman spectroscopies, to examine chemo-structural relationships has been essential to assist the determination of crystallographic information, such as the occupancy of octahedral and tetrahedral sites, and they have also proven extremely useful in relating

Developments in Clay Science, Vol. 8. http://dx.doi.org/10.1016/B978-0-08-100355-8.00007-2

DCS, 978-0-08-100355-8

B978-0-08-100355-8.00007-2, 00007

chemo-structural properties to many of the macroscopic or materials properties of smectites.

p0015 IR spectroscopy lends itself particularly well to the question of structural chemistry and, specifically, the occupancy of various ions in the structure of smectites, because all the octahedral cations present within the structure are a constituent of at least one OH-sharing pair. Thus the IR spectra of smectites are rich in information regarding the actual octahedral cations present and how they are related to their nearest neighbours through shared OH bonds. In addition, as will be explained in more detail below, the vibrational frequencies at which OH-sharing octahedral pairs absorb are affected by the identity of next-nearest neighbours, which while adding complexity to spectral interpretations, also adds further richness of information regarding the actual occupancies with the octahedral, and to some extent, the tetrahedral sites.

p0020 In the next section, some general considerations regarding the state-of-the-science about smectite structures are briefly reviewed. Then, various methods used to interpret IR spectroscopy such as bond valence, reduced mass and ionic size are described in detail.

s0010 7.2 OCTAHEDRAL STRUCTURES OF SMECTITES

p0025 Based on X-ray powder diffraction analyses, enough is known about the structures of many clay minerals to enable detailed analysis of IR spectra, which in turn can assist in refining structures based on chemical analyses. The IR spectrum is sensitive to the next nearest neighbour environment of OH-sharing octahedral cations (Figs. 7.1–7.3), but this has been used to assist in quantifying the octahedral occupancies in only a few cases.

s0015 7.2.1 Di- and Tri-octahedral Structures of Smectites

p0030 All octahedral arrays of clay minerals have two symmetrically inequivalent octahedral sites (Fig. 7.1): M1 and M2, and there are two M2 sites for each

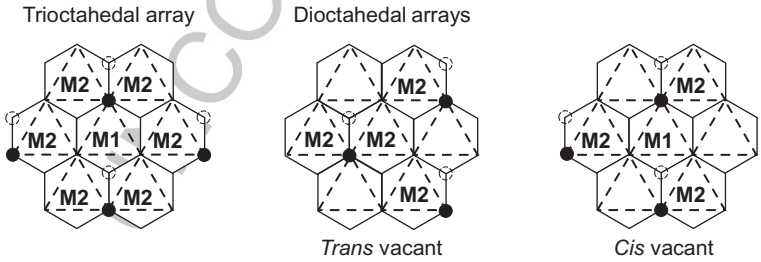

f0005 **FIG. 7.1** The octahedral arrays of smectites. In trioctahedral structures, all octahedral sites are filled with mostly divalent cations. In dioctahedral structures, only two of the three sites are filled, giving *cis*-vacant and *trans*-vacant variants. The tetrahedaral sheets are not shown for clarity. The black filled circles represent hydroxyls at the front face, while the dashed circles represent the hydroxyls at the back face of the octahedron.

B978-0-08-100355-8.00007-2, 00007

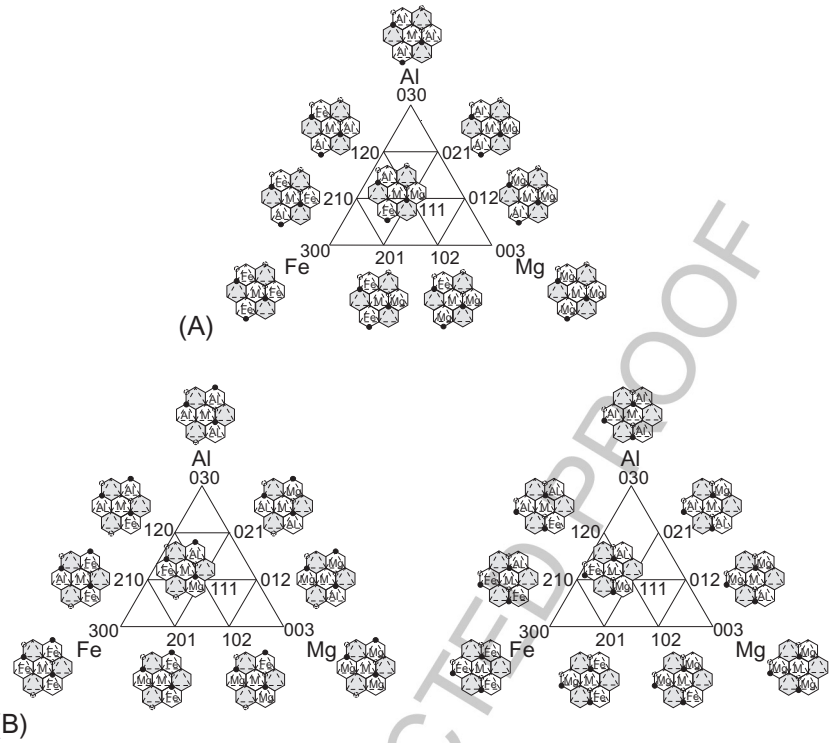

f0010 **FIG. 7.2** (A) Ternary diagrams representing 10 (where M is either Fe, Al or Mg) of the M2(*xyz*) arrays for Fe, Al, Mg occupancies of the possible 72 arrays for *trans*-vacant structures. (B) 10 M2(*xyz*) (left) and M1(*xyz*) (right) arrays each of the possible 144 arrays for *cis*-vacant dioctahedral smectites.

M1 site. The M1 sites are *trans*, whereas the M2 sites are *cis*, with respect to the position of the hydroxyl groups to which at least two octahedra share bonds. Within the classification scheme, there exist *dioctahedral* and *trioctahedral* structural types. In the trioctahedral structures, all three sites are filled with generally divalent cations (Fig. 7.1). Therefore each octahedral site shares an edge with six other octahedral sites as well as corners with tetrahedral sites. Each M1 cation shares one OH with two M2 cation sites and the other OH with two other M2 cation sites, and each of these pairs of M2 sites share edges. Each OH is thus linked to three neighbouring octahedral cations. In the dioctahedral structures, each octahedral cation site shares an edge with three other octahedral cation sites; the other octahedral sites being vacant (Fig. 7.1). Because only two of the three octahedral sites of the formula unit are filled with generally trivalent cations, two symmetry independent variants exist. *Cis*-vacant structural variants have cations occupying the M1 site as well as one M2 site, so each M1 site shares edges with three M2 sites, with two of which it also shares an OH. The *cis*-vacant smectites are generally represented by smectites of intermediate composition, such as montmorillonites and ferrian

B978-0-08-100355-8.00007-2, 00007

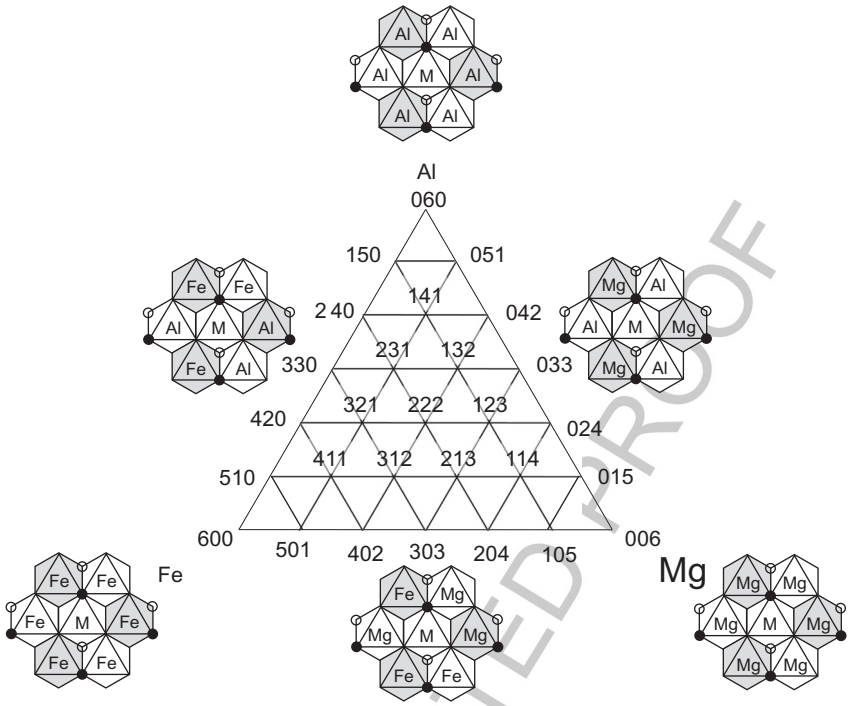

f0015 **FIG. 7.3** A ternary diagram showing some of the many possible M1(*xyz*) (where *x*, *y* and *z* are integers that sum to 6) occupancy arrays in trioctahedral smectites. In this representation, Fe is assumed to be in the ferrous, divalent (Fe^{2+}) oxidation state, and the presence of Fe^{3+} would necessarily increase the complexity. The system can be duplicated for the M2(*xyz*) arrays, where each M2 site has 3 M2 and 3 M1 nearest (*xyz*) neighbours.

(referred to also as ferruginous) smectites having both Fe^{3+} and Mg substitutions in the octahedral sheet. Only the two M2 octahedral sites are occupied in the *trans*-vacant structural variants, so each M2 cation site shares edges with three other M2 sites and both OH with only one of these. The *trans*-vacant smectites are generally represented by the end-member compositions where tetrahedral substitution is high, like nontronites and beidellites, but in ferrian smectites the probability of *trans*-vacant structures increases with octahedral Fe^{3+} content (Emmerich et al., 2009; Wolters et al., 2009; Emmerich, 2013).

p0035 It follows then, that a major advantage for studying smectite structures by IR is due to the fact that hydroxyl groups are shared by at least two octahedral cations. Thus absorption bands associated with OH can be assessed quite quantitatively, as described below. However, in dioctahedral smectites, a major limitation of IR spectroscopy is that octahedral cation pairs exist in *trans*-vacant structures that do not share hydroxyl groups. In addition, corner-sharing tetrahedral cations can induce differences in the mass of the vibrating unit and/or charge that influence the positions of OH-sharing octahedral absorbencies.

B978-0-08-100355-8.00007-2, 00007

s0020 7.2.2 Site Occupancy within a Ternary Fe-Al-Mg Field

p0040 Smectites normally have three major cation occupancies in the octahedral sites: Al, Fe, and Mg and thus depicting the chemistry by means of ternary diagrams is highly useful. Cashion et al. (2008, 2009, 2011) and Gates and Cashion (2014) developed a systematic means to identify potential nearest neighbour cation arrangements within the octahedral sheet. Originally developed to assist in the interpretation of Mössbauer spectra, it has proven to be a useful tool to assist in determining occupancies from IR spectra. It is further developed herein in its most general form.

p0045 Consider that within dioctahedral structures, each octahedral cation has three nearest neighbours (possibly Fe, Al or Mg) in the octahedral arrays of the common natural clay minerals. The details of the distribution surrounding the central cation, M, can be captured by the use of integers, which must sum to 3, representing, respectively octahedral Fe, Al and Mg atoms in nearest neighbour environments, *viz*, Ms(*xyz*), where *s* refers to the specific octahedral site (1 or 2 in smectites; 1, 2 or 3 in e.g. sepiolites). For example, in a dioctahedral smectite Al2(120) would represent an Al atom in an M2 site surrounded by 1 Fe and 2 Al atoms in adjacent edge-sharing octahedra within the trigonal array of the octahedral sheet. Note that in this example the M2 Al would share edges with 3 M1 octahedral cations in *cis*-vacant structures, but with 3 M2 octahedral cations in *trans*-vacant structures. The system, represented as ternary diagrams for the *cis*- and *trans*-vacant dioctahedral smectites, is given in Fig. 7.2.

p0050 For the dioctahedral series, there are potentially 24 symmetrically independent octahedral arrays available for each central cation M. Many of the non-redundant sites in both *cis*- and *trans*-vacant structures will only be observed as broadening or shifts in the main absorbance feature due to changes in the reduced mass of the next nearest neighbour (see Section 7.3.4). Application of the normal (random) distribution theorem (Gates and Cashion, 2014) to the chemistry of the dioctahedral smectites indicates that many of the independent arrays, depending on the specific chemistry of the considered smectite, will be of such low proportion that they can be neglected.

p0055 For the trioctahedral series (Fig. 7.3), due to (mostly complete) occupancy of all sites, there are many more possible outcomes, because Fe can be present in its ferric, trivalent (Fe^{3+}) as well as its ferrous, divalent (Fe^{2+}) state. In addition for many saponites, the octahedral charge may be quite low, or even positive, due to the presence of trivalent cations, and this is usually compensated by the presence of Al for Si substitution in the tetrahedral sheets. As for the dioctahedral arrays, many of the Ms(*xyz*) arrays in Fig. 7.3 can be neglected due to structural-chemical constraints. For example, Ms(600), Ms(060) or even Ms(330) can be neglected if M = Al or if all Fe is present as Fe^{3+}. Of course, if M is Mg and Fe is Fe^{2+}, then M1(123) is a highly

B978-0-08-100355-8.00007-2, 00007

probable array. Note that the sum of x, y and z is nominally 6 for trioctahedral, although the presence of some vacancies (□) can also be incorporated. Q5

p0060 The systematic representation explored above can be expanded to include all the tetrahedral cation nearest neighbours as well (Cashion et al., 2009, 2011), yielding Ms(xyz)Si(t)Al($8-t$), where t represents a number from 1 to 8 (for the $O_{20}(OH)_4$ unit cell). For kaolinite, a site label such as Al2(030) Si(3)Al(1) could be distinguished also by the presence of inner and inner-surface OH, or by the additional presence of nearby interlayer water in halloysite. Thus it should be appreciated that for the di- and tri-octahedral structures the number of symmetrically independent sites can become quite large.

p0065 Similar, but considerably more complex, octahedral occupancy arrays can be considered for palygorskite and sepiolite (Fig. 7.4). These non-swelling 'ribbon' clay minerals consist of discontinuous octahedral arrays linked by modulated sheets of tetrahedra (Serna et al., 1977a; Brigatti et al., 2013a,b), Q6 Q7 resulting in three symmetrically independent octahedral sites: M1 and M2, which are the same as, respectively, the *trans* and *cis* sites in smectites, but also an M3 site, which has two coordination-bonded water molecules extending into the zeolitic channels (Fig. 7.4). Thus in sepiolite (trioctahedral structure), there would exist M1 having 4 M2 and 2 M3 (xyz) nearest neighbours, M2 having 2 M1, 2 M2 and 1 M3 (xyz) and M3 having 2 M3 and 1 M1 (xyz) neighbours. For idealised monoclinic palygorskite (dioctahedral structure), where the M1 site is vacant, each M2 site has two M2 and one M3 neighbours

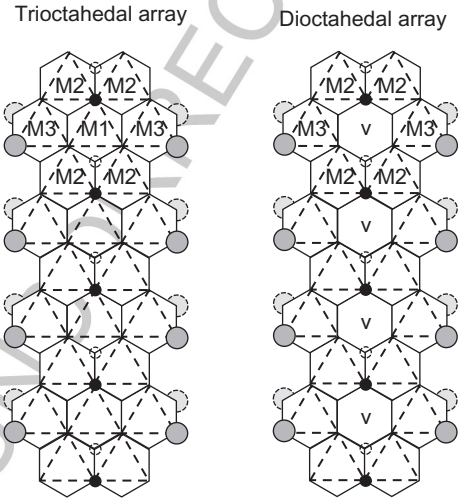

f0020 **FIG. 7.4** The idealised trioctahedral and dioctahedral arrays of, respectively, orthorhombic sepiolite and monoclinic palygorskite. As in Fig. 7.1, the small filled circles represent OH at the upper octahedron face and small dashed circles OH at the back octahedron face. Large filled and dashed circles represent coordination-bonded H_2O at the edges of the octahedral extending within the zeolitic channels.

B978-0-08-100355-8.00007-2, 00007

and each M3 has two M2 (*xyz*) neighbours. The introduction of the periodically inverted tetrahedral sheet, Al for Si substitution within the tetrahedral sheet, as well as the presence of coordination-bound water within the zeolitic channels, results in quite diverse possible occupancies.

p0070 As in the dioctahedral and trioctahedral arrays of smectites, there are limits to the chemical makeup of stable compositions in palygorskite and sepiolite. For example, trivalent cations such as Al or Fe^{3+} are typically only found in the M2 sites, but divalent Mg or Fe^{2+} can be found to be in any of the three sites (Gionis et al., 2006). The bound water is strongly associated with octahedral Mg (Serna et al., 1977a) and has discreet OH stretching, overtone and combination modes (Clark et al., 1990; Gionis et al., 2006, 2007). Thus, in addition to the sites for OH-sharing pairs, sites can be considered for water-bonding to an M3 cation. IR (and Raman) spectroscopies are well placed to assist in the continued discussion regarding the di-trioctahedral character of these minerals (Cases et al., 1991; Stathopoulous et al., 2011; Chahi et al., 2002). Q8

s0025 7.3 EFFECT OF CHEMISTRY ON THE PRESENCE AND POSITION OF BANDS

p0075 Vibrational spectroscopy lends itself well to the study of site occupancy in clay minerals because collection of a single spectrum normally probes many millions of 'unit cells', each of which form part of larger (and contain many) vibrational units. Thus if our models of the crystal structure of smectites and other clay minerals hold, then vibrational spectroscopy probes the local structure, averaged over those many millions of unit cells. The importance of high quality IR spectra as well as sound chemical data on the same samples cannot be overstated. The accuracy and precision of site occupancy determination in smectites can only be as good as the chemical analysis and spectroscopic data. Assuming that the chemical data is accurate then it falls to the spectroscopist to collect the best possible spectra and conduct appropriate treatments of the spectra for analysis. For details of some of these spectral pre-treatments, see Chapter 4 in this volume. A fundamental understanding of spectroscopic selection rules also underpins our ability to quantify the structural chemistry of clay minerals.

p0080 Many earlier works were important in empirically assigning absorption bands to structural features (e.g. Stubičan and Roy, 1961; Vedder, 1964; Goodman et al., 1976; Velde, 1983; Robert and Kodama, 1988; Slonimskaya et al., 1986; Decarreau et al., 1992; Post and Noble, 1993; Madejová et al., 1994; Besson and Drits, 1997a,b; Bishop et al., 1999; Petit et al., 1999b) Q9 although some assignments are still under scrutiny (e.g. Gates, 2008; Bishop et al., 2011; Petit et al., 2015). There have been two main empirical approaches to quantifying structural chemistry from the IR spectra: band decomposition and spectral derivative intensities, both of which will be discussed in detail.

B978-0-08-100355-8.00007-2, 00007

p0085 For dioctahedral smectites, starting with the initial research of Slonimskaya et al. (1986), Muller et al. (1991), Madejová et al. (1994) and Zviagina et al. (2004) have shown how the IR active OH stretching (υ(OH)) band can be used to provide quantitative information on the average occupancies of OH-sharing octahedra. Petit et al. (2004a) detailed how this information could be applied to trioctahedral talc and Vantelon et al. (2001), Gates (2008) and Petit et al. (2016) expanded this treatment to the bending (δ(OH)) bands, while Petit et al. (1999b, 2015, 2016) and Gates et al. (2002) expanded it for the NIR combination bands, for many different smectites. The effect of tetrahedral substitution on the OH-sharing octahedral cation bending bands has been quantified for nontronites (Gates et al., 2002; Gates, 2008; Baron et al., 2016a), but as of yet, not for other smectites due to the difficulty in assigning octahedral sites with this method alone.

s0030 7.3.1 Reduced Mass

p0090 As detailed in Section 7.2, most octahedral cations of smectites and other clay minerals are bonded to one or more OH, and since the O–H bond is strongly IR active, IR spectroscopy has become a valuable tool in determining octahedral site occupancy. Among the earliest explanations of the effects of chemistry on the positions of υ(OH) or δ(OH) bands relates to the reduced mass of the OH-sharing cations. The vibrational frequency of any given υ(OH) or δ(OH) (and presumably υ(OH)+δ(OH) combination band) is related to the force constant (k_{OH}) of the bond and the reduced mass (μ_{OH}) of the vibrating dipole through the well-known expression

$$\upsilon(\mathrm{OH})\ (\text{or}\ \delta(\mathrm{OH})) = \frac{1}{2\pi c}\left(\frac{k_{\mathrm{OH}}}{\mu_{\mathrm{OH}}}\right)^{1/2} \tag{7.1}$$

where c is the speed of light. If the force constant is considered to be constant (the veracity of this assumption will be discussed shortly) then the vibrational frequency is inversely proportional to the reduced mass. Thus, absorption frequencies for $\upsilon\left(\mathrm{Fe}^{3+}{}_2\mathrm{OH}\right)$ are generally lower than those for $\upsilon(\mathrm{AlFe}^{3+}\mathrm{OH})$ or $\upsilon(\mathrm{Al_2OH})$, both of which should be lower than υ(AlMgOH).

p0095 Eq. (7.1) has been used empirically (e.g. Besson and Drits, 1997b; Zviagina et al., 2004; Gates, 2008) to identify the frequency of OH-sharing octahedral cation absorption features as well as to predict potential unknowns in the Al–Fe–Mg (Fe being Fe^{3+} or Fe^{2+}) series of dioctahedral smectites (e.g. Fig. 7.5A). Unfortunately, this straightforward approach does break down, most especially in the υ(OH) region of smectites. For example, Zviagina et al. (2004) observed in some instances that $\upsilon(\mathrm{AlFe}^{3+}\mathrm{OH})$ reside at higher frequencies than $\upsilon(\mathrm{Al_2OH})$. Possible causes for this breakdown will be discussed further.

p0100 One useful approach to negate the effect of adsorbed H_2O on interfering with the υ(MOH) region is to calculate the second derivative (Fig. 7.6).

B978-0-08-100355-8.00007-2, 00007

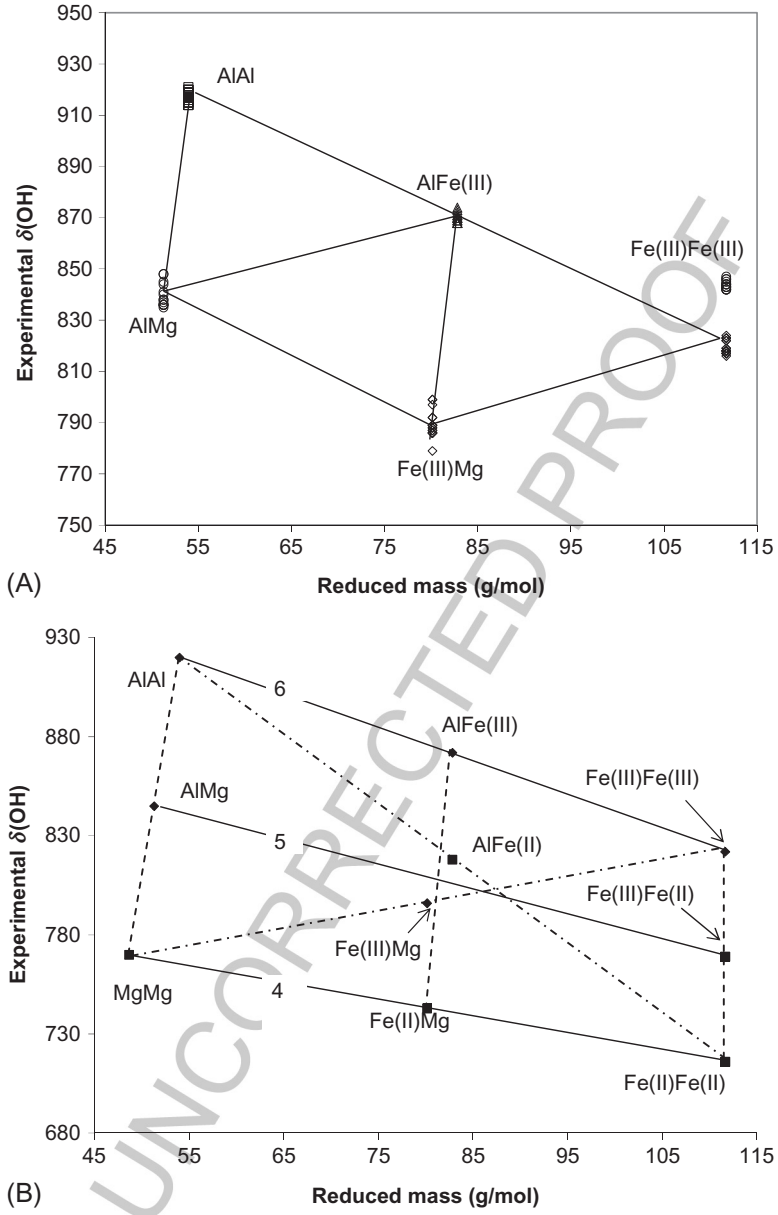

f0025 **FIG. 7.5** (A) Relationship between vibrational frequency of the δ(OH) vs. the reduced mass of the octahedral cation pair in dioctahedral smectites. (B) The same relationship determined for Q1 montmorillonites, as influenced also by the valence sum. *Redrawn from Gates, W.P., 2008. Cation mass—valence sum (CM-VS) approach to assigning OH-bending bands in dioctahedral smectites. Clays Clay Miner. 56, 10–22.*

B978-0-08-100355-8.00007-2, 00007

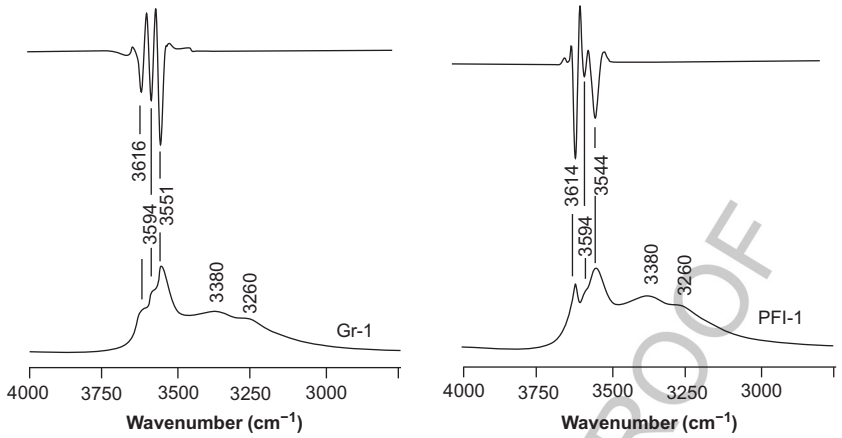

f0030 **FIG. 7.6** MIR spectra of two palygorskite samples studied by Gionis et al. (2006) depicting the υ(MOH) overlapped by $\upsilon(H_2O)$. The second derivative assists in determining the location of the υ(MOH). *Redrawn from Gionis, V., Kacandes, G.H., Kastritis, I.D., Chryssikos, G.D., 2006. On the structure of palygorskite by mid- and near-infrared spectroscopy. Am. Miner. 91, 1125–1133.*

This approach has been exploited by Gionis et al. (2006, 2007) and Chryssikos et al. (2009) to make unambiguous assignments of various OH-sharing octahedral cation pairings (or triads) within the structures of palygorskites and sepiolites to better understand their structural chemistry (see Section 7.4.3)

s0035 ## 7.3.2 Bond Strength (Valence)

p0105 The OH groups of hydroxyl-sharing cation pairs of the same (e.g. Fe^{3+}, Fe^{2+}) or similar (e.g. Al, Mg) mass are observed to have different vibrational frequencies that are directly related to their bond valances. The explanation is based on the bond-valence/bond-length concept originated by Pauling (1929) where decreasing bond valence of the OH-sharing octahedral cations leads to longer bond lengths with the shared bridging oxygen, and therefore allow the O–H bond strength to increase. Increased bond strength in the O–H results in an increased vibrational frequency. Earlier works (e.g. Vedder, 1964; Robert and Kodama, 1988) had reported trends between absorption frequencies and the bond valence. Besson and Drits (1997a,b) confirmed that when the valence sum of the OH-sharing octahedral cation pairs through the bridging oxygen is decreased, as for example Al_2OH vs. AlMgOH, it resulted in an increased bond strength of the O–H and increased frequencies for υ(OH).

p0110 The effect of bond valence has helped to explain some, but not all, of the exceptions evident in the reduced mass approach (see Section 7.3.1). For example, for $\upsilon(AlFe^{3+}OH)$ bands to reside at higher frequencies than an $\upsilon(Al_2OH)$ band, the O–H bond in the former pair must have a higher bond

B978-0-08-100355-8.00007-2, 00007

valence, and thus a higher bonding constant k_{OH}, associated with it (Zviagina et al., 2004). These authors assigned the high frequency $\upsilon(AlFe^{3+}OH)$ to OH-sharing cation pairs within a pyrophyllite-like domain where the lack of surface charge minimised the H-bonding effect of the O–H with oxygens within the vacant octahedral site, resulting in an increased valence sum of the O–H bond (see Section 7.3.4).

s0040 ### 7.3.3 Reduced Mass—Valence Sum

p0115 The position of the specific υ(OH) or δ(OH) has been shown to be modified by the valence sum of the octahedral cation pair involved, which for the series concerned (Fe^{3+}, Al, Fe^{2+}, Mg) is either 4, 5 or 6. (Fig. 7.5B). The presence of divalent Mg, which is approximately the same mass as trivalent Al, decreases the resulting vibration frequency of υ(OH) (Besson and Drits, 1997a,b; Zviagina et al., 2004) and δ(OH) (Gates, 2008). This combined reduced mass-valence sum approach to interpret IR spectra of smectites brings together two of the factors considered most influential in determining vibrational frequency and has been applied previously by many researchers (e.g. Slonimskaya et al., 1986; Clark et al., 1990; Madejová et al., 1994; Petit et al., 1997) and perhaps intuitively by many others. Q14

p0120 For the most natural smectites (i.e. of Al–Fe^{3+}–Mg octahedral series, with perhaps some Fe^{2+}), any M^aN^b cation pair (where M and N are the cation and superscript *a* and *b* are the valence) the position of the OH bands could be predicted from the positions of known bands of like-cation pairs through the relation:

$$M^aN^b\left(cm^{-1}\right) = \frac{\left(M_2^a + N_2^b\right)}{2}\left(cm^{-1}\right) \tag{7.2}$$

p0125 The following simple rules (Gates, 2008) apply:

o0005 **(i)** For OH-sharing cation pairs with the same valence sum, increased reduced mass results in decreased vibrational frequency;

o0010 **(ii)** For OH-sharing cation pairs with the same reduced mass, increased valence sum results in increased vibrational frequency;

o0015 **(iii)** Simultaneous increase in both reduced mass and valence sum of OH-sharing cation pairs results in increased vibrational frequency;

p0145 Application of Eq. (7.2) and the above rules enabled the development of the relations depicted in Fig. 7.6. These relationships hold only for the υ(OH) or δ(OH) (presumably the υ(OH)+δ(OH) combination bands also) of natural dioctahedral smectites within the Al–Fe–Mg solid solution series. Some evidence suggests that they also apply to the synthetic Ni^{2+} smectites. As has only very recently been shown (Petit et al., 2016), these relationships do not hold for synthetic smectites containing Ga (see Section 7.3.5).

B978-0-08-100355-8.00007-2, 00007

p0150 Gates (2008) used this approach to show that Mg clustering does indeed exist in the dioctahedral smectites, which was previously suspected by others (e.g. Decarreau et al., 1987b). Cashion et al. (2008) were better able to interpret the Mössbauer spectra of some ferrian smectites only if Mg clustering, and its effect on layer charge distributions, were considered. Q15

s0045 7.3.4 Effects of Next Nearest Neighbour Isomorphic Substitution

p0155 Some interesting observations have come from the application of the reduced mass-valence sum approach to well-studied samples. As discussed in detail by Besson and Drits (1997a) and by Gates (2005) isomorphic substitutions within the structure affect the strength of the O–H bond through the influence on the bridging oxygen (Robert and Kodama, 1988) and result in observed shifts in υ and/or δ vibrations of $M^a{}_2OH$, or M^aN^bOH pairs where nearest neighbour compositions differ (Besson and Drits, 1997b; Zviagina et al., 2004). As mentioned in the previous Section 7.3.2, the presence of segregated M^aN^bOH pairs within local domains in dioctahedral smectites lacking isomorphic substitution gives rise to $\upsilon(Al_2OH)$ bands at higher frequencies than those where some substitutions have occurred nearby. The mechanisms involved in changing the frequency of the O–H mode by isomorphic substitutions in the dioctahedral smectites are:

o0020 **(i)** Decreasing the valence sum of the OH-sharing octahedral cation pair directly leads to an increased valence sum of the O–H bond and a resulting increased vibrational frequency. The converse is true: the O–H bond valence sum will decrease if the valence sum of OH-sharing octahedral cations increases, resulting in a decreased vibrational frequency of the structural OH band.

o0025 **(ii)** Lower valence substitutions (e.g. Mg for Al) in any of the two (*trans*-vacant) or three (*cis*-vacant) octahedral sites (Fig. 7.7A), or in any of the 4 tetrahedral sites (e.g. Al for Si) opposite the octahedral vacancy (Fig. 7.7B) result in increased H-bonding across the ditrigonal cavity. This leads to a decrease in the O–H bond valence and a decrease in the vibrational frequency of the structural OH band.

p0170 Gates (2005) used this approach to make some sense of the positons of δ(OH) and υ(OH) + δ(OH) bands of 35 dioctahedral smectites with a large range in octahedral compositions. Montmorillonites with high octahedral Mg substitutions (Fig. 7.8) tended to have lower frequencies (near 915 cm^{-1}) associated with $\delta(Al_2OH)$ and smectites with a high degree of tetrahedral Al substitution (beidellites) had an additional band at higher wavenumber (from 935 to 960 cm^{-1}) attributed to $\delta(Al_2OH)$ sites that are more similar to beidellites (Kloprogge et al., 1990a; Kloprogge, 2006). The former result can be explained by a greater degree of H-bond across the ditrigonal cavity with the oxygen anionic network bonded to Mg, which, while increasing the Q16 Q17

B978-0-08-100355-8.00007-2, 00007

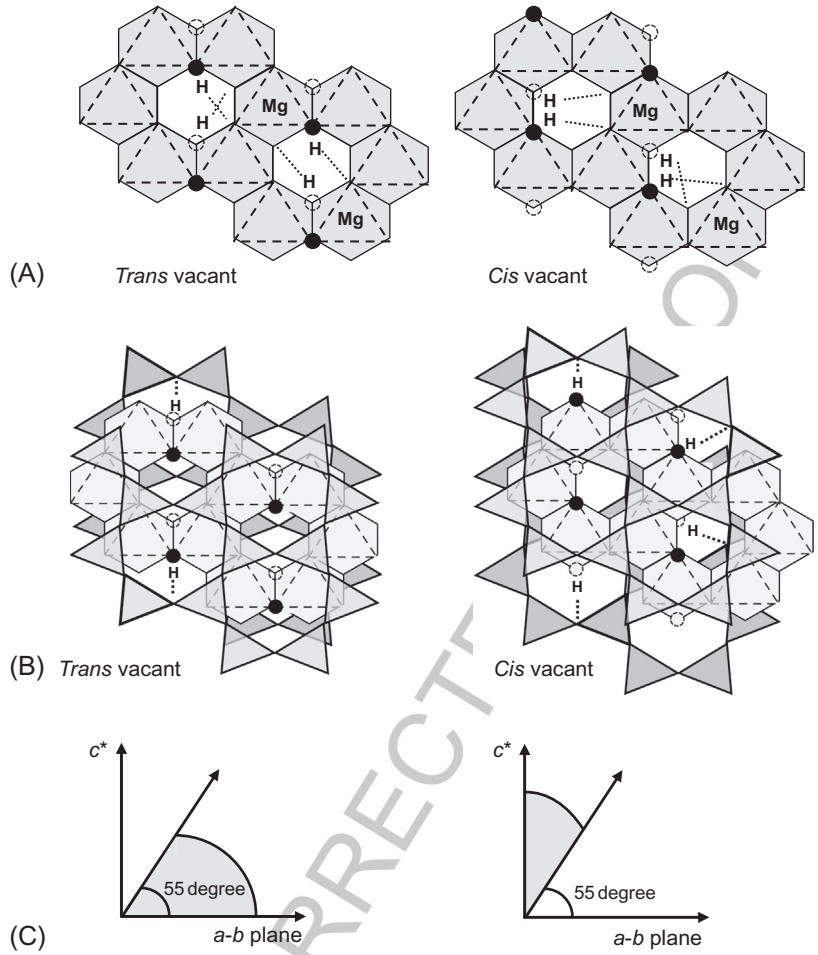

f0035 **FIG. 7.7** (A) Dioctahdral arrays depicting how Mg for Al substitutions result in increased H-bonding across the ditrigonal vacancy. (B) Al substitutions for Si in tetrahedral cause greater variation in H-bonding in *cis*-vacant compared to *trans*-vacant structures. Isomorphic substitutions resulting in layer charge depicted in (A) octahedral by 'Mg' labels and (B) in tetrahedral by thick outlines. (C) Tilt angles of the O–H vector (either stretching, bending or deformation) are $<55^{degree}$ where octahedral Mg substitutions dominate (left) or $>55^{degree}$ where tetrahedral substitutions dominate (right).

H-bond strength, reduces the O–H bond valence by forcing the OH vector to both bend and stretch more in line with the layer plane (Fig. 7.7C). The latter result can be explained by the stronger H-bond with the oxygen network due to Al for Si substitutions in the tetrahedral sheet, which forces the OH vector to bend and stretch at a steeper angle with respect to the layer plane (Fig. 7.7C).

B978-0-08-100355-8.00007-2, 00007

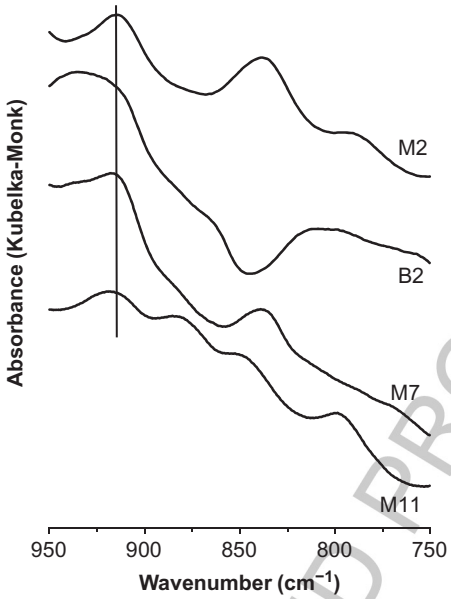

f0040 **FIG. 7.8** The effect of isomorphic substitutions of Mg for Al on the positions of the Al_2OH band in montmorillonites and beidellites. Labels refer to the smectites studied by Gates (2005). Vertical line is at 915 cm^{-1}, typical of $\delta(Al_2OH)$ of montmorillonites. Note that for montmorillonites with less octahedral Mg (i.e. M11, M7) the position of the $\delta(Al_2OH)$ band shifts to higher frequency compared to montmorillonites with high Mg contents (i.e. M2), more similar to beidellites (i.e. B2). NB, the $\delta(M^aN^bOH)$ spectrum of M11 is broadened by the much greater concentration of octahedral Fe^{3+} than is present in the other smectites.

p0175 The effect of isomorphic substitution on the orientation of the OH bending vector is clearly shown in the polarised synchrotron IR spectra displayed in Fig. 7.9, where self-supporting films were measured with the film plane at 0, 20, 35, 50 and 60 degree with respect to the electric field vector of the IR beam, which itself is orthonormal to the beam direction (see Manceau et al., 1998 for details of this type of experimental approach). Isotropic (i.e. invariant with measurement angle) spectral intensities would be expected for OH bending deformation vectors inclined $\approx$55 degree with respect to the film plane. For OH deformation vectors inclined at angles steeper than 55 degree, a positive anisotropic trend (increased spectral intensity with increasing measurement angle) would be observed, but a negative anisotropic trend in intensity would be observed for OH vectors inclined at angles <55 degree. Tetrahedral substitutions of 0.23 Al in ferrian smectite (F5) cause the $\delta(Al_2OH)$ and δ(AlFeOH) O–H vector to be inclined at a steeper angle, but little effect is observed on the Fe_2OH band for the Clausthal Zellerfeld nontronite (N12) with 0.92 tetrahedral Fe^{3+} (and 0.04 Al) substitutions. The strong positive anisotropy of the Fe-O out-of-plane deformation δ(FeO) band attests to the high degree of alignment of nontronite particles

B978-0-08-100355-8.00007-2, 00007

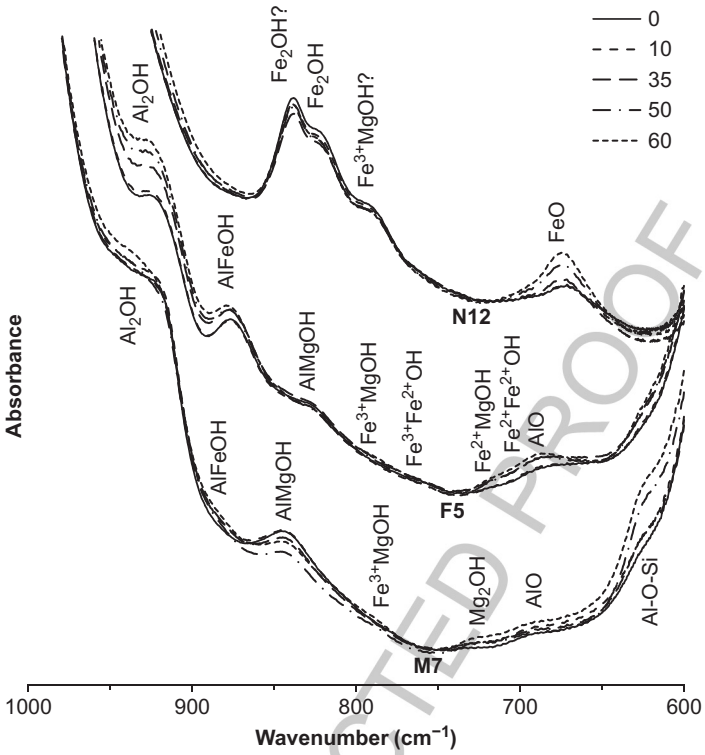

f0045 **FIG. 7.9** The effect of isomorphic substitutions in tetrahedral and octahedral sites on the orientations of the $\delta(M^aN^bOH)$ bands in montmorillonite (M7), Fe smectite (F5) and nontronite (N12) as observed from polarised Synchrotron IR spectra of oriented films. Self-supporting oriented films were inclined at the angles given relative to the electric field vector, which is >99% polarised orthonormal to the beam direction. Spectra presented are co-additions of 10 scans referenced to dry N_2 using a mylar beam splitter and liquid N_2 cooled MCT detector, operating at 0.5 cm^{-1} resolution on the Far-IR high resolution beamline of the Australian Synchrotron. *Assignments based on Gates, W.P., 2008. Cation mass—valence sum (CM-VS) approach to assigning OH-bending bands in dioctahedral smectites. Clays Clay Miner. 56, 10–22.*

within the films. Thus, tetrahedral Fe^{3+} for Si substitutions apparently do not influence the H-bond across the ditrigonal cavity to the same extent as Al (as depicted in Fig.7.7B), and this is in line with differences in the acidity of these cations.

p0180 The Mount Binjour montmorillonite (M7), which has a layer charge, *X*, of 1.23 e^- per O_{22} equivalents, is at the upper end of layer charge for dioctahedral smectites (Gates, 2005). This smectite has a substitution of 0.52 Al per unit cell in the tetrahedral sheet, which only marginally increased the OH bending deformation vector inclination (Fig. 7.9) for $\delta(Al_2OH)$ and δ(AlFeOH) compared to that observed for F5. However, Mg for Al

B978-0-08-100355-8.00007-2, 00007

substitutions in the octahedral sheet strongly decreased the bending vector inclination for δ(AlMgOH) in M7 but had little effect on that for F5. These latter effects indicate that for M7, tetrahedral Al substitutions probably occur in close proximity to sites of octahedral Mg substitutions (i.e. Al(021)Si_7Al and Al(111)Si_7Al) and thus the resulting H-bond is strongly influenced by octahedral substitutions. To the best of our knowledge, these data represent the first published confirmation of the effects of the location of an isomorphic substitution on the orientation of the OH stretching vectors associated with specific OH-sharing octahedral cation pairs originally postulated by Besson and Drits (1997a), Zviagina et al. (2004) and Gates (2005).

p0185 For the $\delta(Fe_2OH)$ band in Fig. 7.9 marked with '?', the previous assignments remain questionable. This band grows in intensity with increasing Fe^{3+} for Si^{4+} substitution, up to about 1 Fe^{3+} per 8 tetrahedral sites (Gates, 2008), but does not exist for synthetic nontronites having more than 1 Fe^{3+} per 8 tetrahedral sites (Baron et al., 2016a). However, determination of the Q18 occupancy (see Section 7.4) appears to require this band to be associated with octahedral Fe. The band indicated as δ(FeMgOH)? for nontronites is too intense to be associated solely with octahedral Mg (Gates, 2005), as shown in the following discussion.

s0050 7.3.5 Ionic Radii Effects—A Generalised Approach

p0190 The reduced mass-valence sum relationship described in Section 7.3.3 breaks down when applied to Ga^{3+} for Fe^{3+} octahedral solid solution series of synthetic smectites (Petit et al., 2016). In this latter case, the positions of υ(OH), δ(OH) and υ(OH)+δ(OH) bands increase in frequency with increases in the reduced masses of $2Fe^{3+}$, $GaFe^{3+}$ and 2Ga OH-sharing octahedral pairs. As depicted in Fig. 7.10, a more generalised relationship, presumably suitable to explain all compositions and one that utilises the average ionic radii of the octahedral cations rather than the reduced mass, has been developed by Petit et al. (2016). Its generality was proven to extend to the Al-Fe series and allowed correct prediction of the position of υ(OH), δ(OH) and υ(OH)+δ(OH) bands of intermediate compositions.

p0195 The M-O bond distance discussed above in Section 7.3.2 represents an indirect measure of ionic radius. The valence state of the metal influences the ionic radius, bond valence and therefore, bond distance. While this explains in part the positions of some known absorbance bands, the lack of large data sets make such relationships difficult to assess. Note that in Fig. 7.10, the relationship for δ(OH) and the average ionic radii of the pair differ from that for υ(OH) (not shown) and this has consequences on the relationship for υ(OH)+δ(OH) (Petit et al. (2016). The υ(OH) bands were used by Petit et al. (2016) initially in developing the respective empirical relationships described above in Section 7.3.1, because the data sets were the most robust.

B978-0-08-100355-8.00007-2, 00007

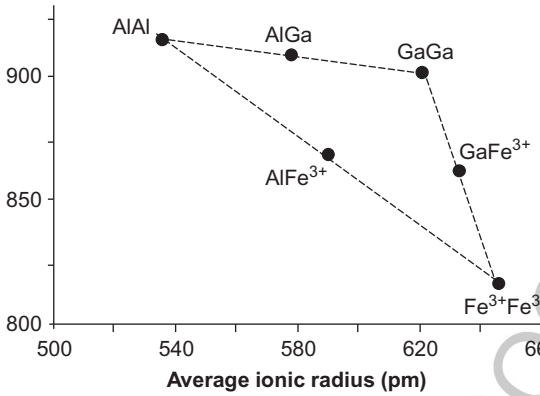

f0050 **FIG. 7.10** The relationship for the position of δ(OH) bands in the Ga–Al–Fe synthetic smectite series as a function of the average ionic radius of the octahedral cation pair. Relations for υ(OH) and υ(OH)+δ(OH) also exist. *Redrawn from Petit, S., Baron, F., Grauby, O., Decarreau, A., 2016. Revisiting the cation mas-valence sum approach to assigning infrared OH-bands in dioctrahedral smectites in the light of new data from synthetic Ga-Fe^{3+} smectites. Vib. Spectrosc. 87, 137–142.*

However, the frequency relationships to ionic radii of the octahedral cation pairs largely explain the occurrence of apparent exceptions, or even opposite responses, of IR absorption bands as a function of reduced mass, bond valence or combined effects.

s0055 7.4 METHODS TO QUANTIFY OCTAHEDRAL OCCUPANCY FROM IR SPECTRA

p0200 NIR and MIR spectra provide useful probes of octahedral occupancy in clay minerals because all OH-sharing octahedral cation pairs contribute to the IR spectrum. As long as appropriate care is taken, useful and accurate complementary information can be gleaned from the IR spectra. As will be discussed further below, the main reason for widespread uptake of this method to determine site occupancy has been due to a lack of unambiguous assignments of some IR active absorbance bands.

p0205 The application of a band decomposition technique and the determination of chemistry has been the more common approach for many decades (e.g. Slonimskaya et al., 1986; Madejová et al., 1994; Frost et al., 2000b; Vantelon et al., 2001; Zviagina et al., 2004; Gates, 2005, 2008; Petit et al., 2004a, 2015, 2016). The application of spectral derivatives has been promoted more recently, largely to the more complex octahedral sheet composition of palygorskites (Gionis et al., 2007; Chryssikos et al., 2009) or Ni-rich lizardites (Baron and Petit, 2016). In both of these approaches; however, successful determinations of clay mineral chemistry from IR spectra have been based on the empirical analysis of multiple samples consisting of a range of spectral Q19

B978-0-08-100355-8.00007-2, 00007

characteristics that could be precisely matched to the chemistry (or other measures) of specific samples.

s0060 ### 7.4.1 Band Decomposition

p0210 The band decomposition method has been used to quantify the chemistry of clay minerals. Some of the more important works have already been discussed in the context of the various models used to understand assignments. Arguably the easiest band decompositions are of the NIR spectra (e.g. Gates et al., 2002; Petit et al., 2004a, 2015; Bishop et al., 2011; Baron and Petit, 2016; Baron et al., 2016a). Compared to MIR bands in the bending/deformation region, these bands are broad, have Gauss character, are often minimally overlapping and generally are not affected by a sloping background. Nor do the NIR combination bands have strong overlapping contributions from other vibrational features that are not related (or not of interest) to chemical quantification, such as the O–H stretching bands associated with adsorbed water in the MIR. Another feature is that the low intensity bands of interest, while often overlapped by strong tails from other bands, are sufficiently resolved to enable their quantification. An example is depicted in Fig. 7.11, where the percentage of integrated intensity based on a random distribution of cations from chemical analysis (Fig. 7.11A) and from decomposition of the NIR spectra (Fig. 7.11B) are compared to the actual percentage of integrated intensity for the occupancy assignments of synthetic talc studied by Petit et al. (2004a). Clearly the NIR spectral decomposition provides a more accurate

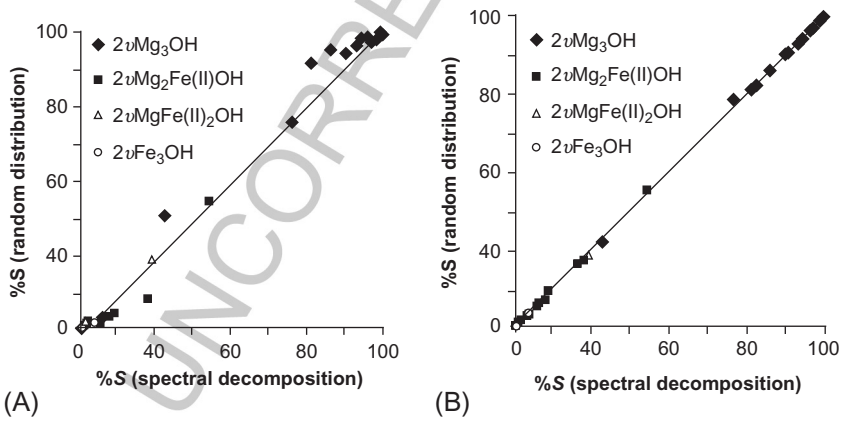

f0055 **FIG. 7.11** Results of spectral decomposition of Mg/Fe(II) talcs depicting the determination of site occupancy from a random distribution from (A) chemical analysis and (B) decomposition of the NIR spectra as detailed in Petit et al. (2004a), vs. the integrated intensity (%S) of the NIR bands (Fig. 5.6A, Chapter 5). *Adapted from Petit S., Martin, F., Wiewiora, A., De Parseval, Ph., Decarreau, A., 2004. Crystal-chemistry of talcs: a NIR and MIR spectroscopic approach. Am. Miner. 89, 319–326.*

B978-0-08-100355-8.00007-2, 00007

determination of the actual site occupancy. A similar finding was observed using the NIR spectra to determine the site occupancy of nontronites (Gates et al., 2002) and synthetic dioctahedral ferrian smectites (Petit et al., 2015, 2016).

p0215 Absorption bands in the OH stretching region, however, are frequently more difficult to decompose because (1) they often occur as strongly overlapping doublets; (2) they are usually overlapped by bands associated with adsorbed water, and (3) the structural *ν*(OH) bands have Gauss character, whereas the intermingling adsorbed water bands generally have Lorentz character. These effects lead to difficulties in detecting, resolving and quantitatively decomposing the less intense bands. Nonetheless, information from these bands are considered to be the most informative regarding the structural-chemistry of the layer silicates (Madejová et al., 1994; Madejová and Komadel, 2001; Frost et al., 2001b; Petit et al., 2004a) and require care to remove, as far as possible the effects of adsorbed water, by either heating/desiccation (see Clark et al., 1990; Cases et al., 1991; Madejová et al, 1994; Gionis et al., 2006, 2007) or by deuteration (Kuligiewicz et al., 2015a,b).

p0220 Decomposition of the bending deformation region (Vantelon et al., 2001; Gates, 2005, 2008) has proven successful for detailed occupancy assignments in dioctahedral smectites, largely because the bands are separated (non-overlapping) in this region. For the montmorillonites and ferrian smectites, most bands have been confidently assigned. A major drawback of decompositions in this region is the fact that these bands are overlain by the strong Si–O stretching band, and the position of this band itself is affected by isomorphic substitution (Madejová and Komadel, 2001) as well as by the hydration state (Yan et al., 1996a). Q20

s0065 7.4.2 Spectral (Second) Derivative

p0225 The application of spectral derivatives for the quantification of IR absorbance bands has been limited to a few studies (Gionis et al., 2007; Chryssikos et al., 2009). The second derivative of an IR spectrum pinpoints, as a negative envelope, the location of narrow band components. It is useful because broad bands and sloping backgrounds are eliminated. The baseline for analysis then becomes the zero-line of the second derivative and the intensities of bands of interest are negative (Fig. 7.12). Within a spectrum, the negative intensities provide a quantitative measure of the chemistry for unambiguously assigned bands. Q21

p0230 Successful application of this method requires high quality spectra because the determination of the second derivative usually results in several tens- or even a hundred-fold increase in the relative noise. Judicious use of smoothing functions (Savitzky and Golay, 1964) can minimise noise, but care must be taken to also minimise the loss of negative intensity, which impairs quantification. Gionis et al. (2007) report that negative intensities of the second

B978-0-08-100355-8.00007-2, 00007

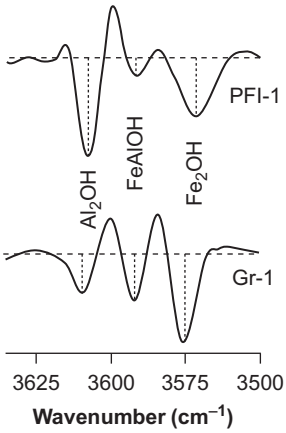

f0060 **FIG. 7.12** The second derivative of the structural υ(MOH) for the same two palyogroskite samples depicted in Fig. 7.5. While the positions of likely bands can be ascertained from the IR spectrum, their unambiguous assignment required the application of the second derivative. The dashed vertical lines represent the relative negative intensities of the υ(MOH) component bands and can be used to quantify composition (see Section 7.4.2). *Redrawn from Gionis, V., Kacandes, G.H., Kastritis, I.D., Chryssikos, G.D. 2006. On the structure of palygorskite by mid- and near-infrared spectroscopy. Am. Miner. 91, 1125–1133.*

derivative of palygorskites were reproducible with 5% error, within acceptable limits of most other methods (Gates et al., 2002). This method may also prove useful in dealing with complex mixtures where overlapping bands of different mineral phases overlap.

s0070 ## 7.4.3 Assigning Occupancies

p0235 The quantitative information from band decomposition and the second derivative intensity analysis can be used to determine the octahedral composition of smectites with a high degree of accuracy. The approach requires accurate integrated intensities of all known M^aN^bOH pairs within the region of interest—and also of the same sort of band (i.e. for either υ(OH) or δ(OH) or υ(OH) + δ(OH), but not mixtures). Then for dioctahedral smectites, the number of octahedral M^a sites, on the typical basis of $O_{20}(OH)_4$, can be determined from (Besson and Drits, 1997b; Gates, 2008):

$$\mathrm{Oct}\,M^a = 4x\left[2xA(M)^a_2OH + \sum\nolimits_n A\left(M^aN^bOH\right)\right] \qquad 7.3$$

p0240 In Eq. (7.3), A is the normalised integrated peak area (or second derivative intensity), n is the number of M^aN^bOH bands observed in the IR spectrum For example, to determine the occupancy of Al, M^a, in montmorillonite, one requires information on A for Al_2OH, AlFeOH and AlMgOH, (as well as any other AlN^bOH pair) as well as n and must be applied iteratively for each

B978-0-08-100355-8.00007-2, 00007

N^b (as M^a) in turn to provide a statistical octahedral assignment. The quantification is normalised to 4 for dioctahedral smectites. Similar expressions can be developed for other clay mineral species.

p0245 A major assumption that is required in order for this methodology to provide quantitative estimates of occupancy, and which has caused (and continues to cause) difficulty is the proper assignment of some of the bands in question. For example in spectra of nontronites, a low intensity band near 750 cm^{-1}, often only observed as a shoulder to the more intense deformation of Fe_2OH (cf. Fig. 7.8) has been previously assigned to δ(FeMgOH) (e.g. Gates, 2005) for montmorillonites and ferrian smectites based on the occurrence of δ(FeMgOH) in the correct frequency range on the application of Eq. (7.3). However, it is now apparent that the full intensity of this band in natural nontronites (Gates, 2008) cannot be solely associated with octahedral Mg as it occurs also in synthetic nontronites free of Mg.

s0075 7.4.4 Comparison to Random Distributions

p0250 Random distribution analysis is a highly useful approach to assist in determining deviations in the measured, or estimated, occupancies. Gates and Cashion (2014) have used this approach to show that most dioctahedral smectites (of the 35 studied by Gates, 2005) having chemistries close to end-member nontronite, montmorillonite or beidellite, have octahedral cation occupancies that can be largely explained by random distributions. For example, deviations from random distributions based on the chemistry of the six nontronites, were observed to indicate enrichments of tetrahedral substitution (Fe(300) $Si_7(AlFe)_1$, Fe(300)$Si_6(AlFe)_2$, Fe(210)$Si_7(AlFe)_1$) and octahedral substitution (Fe(210)Si_8). These sites (and Fe(300)Si_8) represented more than 80 percent of all possible sites. Most of the remaining 20 percent of the sites were made up of higher levels of tetrahedral substitution, with or without one octahedral Al^{3+} for Fe^{3+} substitution per unit cell. For the single ferruginous smectite (SWa-1) studied, these five sites only represented 60 percent of the available sites, largely due to the increase octahedral Mg content.

p0255 Intermediate compositions, as for the ferrian smectites, or compositions with elevated Mg, as in some montmorillonites and ferrian smectites, tend to deviate from random distribution (Gates, 2008). Past research observed deviations from random distributions, but ascribed that it may have been due to the intermixing of dioctahedral (nontronites) and trioctahedral (Ni-rich) smectites (Decarreau et al., 1987b; Mano et al., 2014). In the specific example of the ferrian smectites studied by Gates (2008), excess Mg and the presence of residual Fe^{2+} resulted in the clustering of sites of OH-sharing divalent cation pairs, such as Mg_2OH, $Fe^{2+}MgOH$ and $Fe^{2+}{}_2OH$.

p0260 While not surprising results in and of themselves, when compared to distributions calculated from IR spectral decompositions (e.g. Madejová et al., 1994; Vantelon et al., 2001; Gates, 2008), or from other methods, such as

B978-0-08-100355-8.00007-2, 00007

X-ray absorption spectroscopy (Manceau et al., 1998) or Mössbauer spectroscopy (Cashion et al., 2009), the results do provide complementary evidence for the correctness of assignments made in the IR.

7.5 CONCLUSIONS AND FUTURE DIRECTIONS

p0265 The determination of the composition of the clay minerals from IR follows basic rules associated with valency, atomic or molecular mass and ionic size. These rules that have been used by mineralogists for nearly a century. Aspects of each of these parameters were initially promoted by Farmer in the 1970s and have been used by many researchers in an attempt to unambiguously identify absorbance bands. For the most part this has been highly successful, and clay mineralogists can understand an enormous amount about a clay mineral of interest 'simply' by study of its IR spectrum. There have been some exceptions, as detailed in this chapter.

p0270 The determination of the chemical occupancy of clay minerals has also come far since Farmer (1997) on the IR spectroscopy of the clay minerals. Q22 The applications demonstrated here mainly for Al, Fe and Mg occupancies in dioctahedral smectites may be extended to other clay minerals, as well as clay minerals containing exotic elements such as Ga and Ni. While nearly all of the advances described above have been empirical in nature, with the advent of molecular dynamics (e.g. Martínez-Alonso et al., 2002a; Cygan et al., 2004; Greathouse and Cygan, 2013; Ferrante et al., 2015; Greathouse Q23 et al., 2016) and calculations of the IR spectra of similar minerals as described in detail in previous Chapters 2 and 6 of this volume, a new generation of exciting advances in this area is about to occur.

B978-0-08-100355-8.00007-2, 00007

Non-Print Items

Abstract

The chemical composition of clay minerals directly influences their infrared (IR) spectra and follows basic rules associated with valence, atomic or molecular mass and ionic size. This fact has been exploited for many decades to assess and unambiguously identify IR absorbance bands, and in the past three decades, to quantify specific site occupancy studying the IR spectrum.

Keywords: IR, Raman, IR spectroscopy, Raman Spectroscopy, Clay mineral, Chemical composition, Structure types, Octahedral sites, Reduced mass, Bond strength, Bond valence, Ionic size, Nearest neighbour

Q4